Bull. Nov. Comp. Center, , (2013), 1–13

Application of a mixed finite element method for solving 2D nonlinear vorticity equation in a variable bottom water basin

V.I. Kuzin, V.V. Kravtchenko

Abstract. Based on the splitting in terms of physical processes and with respect to time and on a finite element method (FEM) as applied to a 2D nonlinear vorticity equation, a scheme with two splitting steps is obtained. For constructing FEM operators at the steps of splitting in terms of physical processes, different types of finite elements are used. In the statement of the problem a special attention is given to the depth of a basin. The efficiency of the scheme was tested for a uniform bottom and for the bottom defined by a smooth function.

Introduction

The problem of determining a plane non-stationary circulation is one among the typical ocean dynamics problems. This initial-boundary value problem is described by a 2D nonlinear vorticity equation. In this paper, we present a scheme for which the splitting combined with a finite element method (FEM) is used. In this case, splitting is carried out at different steps of constructing a numerical model, including both splitting in terms of physical processes allowing linearization of the initial problem, and further splitting with respect to time of one of the FEM operators obtained. For constructing FEM operators at the steps of splitting in terms of physical processes, different types of finite elements are used. Hence, it appears possible to essentially reduce the number of grid points in a numerical scheme when passing from one splitting step to another. At the second step, for solving the linear stream function equation, the conforming piecewise linear finite elements are used. At the first step, corresponding to the vorticity advection and diffusion, the non-conforming finite elements are used. Finite elements of such a type were introduced by M. Crouzeix and P.A. Raviart [1] for solving the stationary Stokes equations. Later these elements were used by B.-L. Hua and F. Tomasset [2] to obtain a noise-free scheme for two-layer shallow water equations. Some of their advantages are listed below. Because of orthogonality we can avoid the lumping procedure at the splitting steps with respect to time. Also, in comparison with the case of conforming finite elements, a smaller number of grid points is used in the FEM scheme obtained. At the same time, on a standard grid, the degrees of freedom in this case increase by the factor of 3 that may improve the accuracy of an FEM

solution. The equations obtained conserve transformation laws for some integral characteristics such as mass and energy with respect to time, which is important for obtaining correct solutions in terms of physical features. Analysis of the FEM operator obtained after using non-conforming finite elements shows that it can be split into two three-point positive semi-definite operators. As compared to the coordinate-wise splitting, the factorization goes along the broken lines connecting mesh points. Apparently, such an approach has not been used yet in the splitting-up theory. On the contrary, in the case of conforming finite elements, there was a splitting into, at least, three operators, including the diagonal direction [3].

An essential problem of using non-conforming finite elements is that an FEM solution does not belong to the space of solvability of the initial problem that demands an additional formal foundation.

1. Statement of the problem

In the domain $Q = \Omega \times (-H(x,y), 0) \times (0,T)$, $H(x,y) \geq H_0 > 0$, let us consider a quasistatic model for the barotropic ocean, i.e., all the thermodynamic effects are neglected, vertical structure of the ocean being considered as uniform $\rho = \rho_0 = \text{const}$:

$$\frac{du}{dt} - fv = -\frac{1}{\rho_0} p_x + \mu \Delta u + (\nu u_z)_z, \tag{1}$$

$$\frac{dv}{dt} + fu = -\frac{1}{\rho_0} p_y + \mu \Delta v + (\nu v_z)_z, \tag{2}$$

$$u_x + v_y + w_z = 0, \tag{3}$$

$$p_z = g\rho. \tag{4}$$

Here the following notations are used:

$$\frac{dU}{dt} = U_t + (U \cdot \nabla)U + wU_z, \quad U = (u,v), \quad \nabla = \Big(\frac{\partial}{\partial x}, \frac{\partial}{\partial y}\Big),$$
$$\Delta u = u_{xx} + u_{yy}, \quad \Delta v = v_{xx} + v_{yy},$$

u, v, w are components of the velocity vector along the axes x, y, and z, respectively, f is the Coriolis parameter, p is pressure, ρ is density, ρ_0 is a representative value of density, μ is the horizontal turbulent viscosity, ν is the vertical turbulent viscosity.

Boundary and initial conditions for (1)–(3):

$$z = 0: \quad \nu u_z = -\frac{\tau_x}{\rho_0}, \quad \nu v_z = -\frac{\tau_y}{\rho_0}, \quad w = 0,$$

$$z = H(x,y): \quad \nu u_z = -R\int_0^H u\,dz, \quad \nu v_z = -R\int_0^H v\,dz, \quad w = U\cdot\nabla H,$$

$$(x,y) \in \partial\Omega: \quad \bar{U}\cdot N = 0, \quad \bar{U} = \frac{1}{H}\int_0^H U\,dz,$$

$$t = 0: \quad U = U^0.$$

Then for the barotropic part of the motion $\bar{U}$, after integration of equation (3) with respect to z from 0 to $H(x,y)$, transformation of the variable $(x',y',z') = \left(x, y, \frac{z}{H(x,y)}\right)$, and integration of equations (1), (2) with respect to z' from 0 to 1 we can obtain the following system of equations (primes are omitted):

$$\bar{u}_t + \bar{U}\cdot\nabla\bar{u} - f\bar{v} - \mu\Delta\bar{u} + R\bar{u} = -\frac{1}{\rho_0}\left(\int_0^1 p_x dz - gH_x\int_0^1 z\rho\,dz\right) + \frac{\tau_x}{\rho_0 H}, \quad (5)$$

$$\bar{v}_t + \bar{U}\cdot\nabla\bar{v} + f\bar{u} - \mu\Delta\bar{v} + R\bar{v} = -\frac{1}{\rho_0}\left(\int_0^1 p_y dz - gH_y\int_0^1 z\rho\,dz\right) + \frac{\tau_y}{\rho_0 H}, \quad (6)$$

$$(H\bar{u})_x + (H\bar{v})_y = 0. \quad (7)$$

Let us consider dimensionless variables

$$x' = \frac{x}{L}, \quad y' = \frac{y}{L}, \quad H' = \frac{H}{H_m}, \quad t' = \frac{U_0}{L}t, \quad U' = \frac{\bar{U}}{U_0},$$

$$f' = \frac{f}{2\Omega_{pl}}, \quad \rho' = \frac{\rho}{\rho_0}, \quad p' = \frac{p}{p_0}, \quad \tau' = \left(\frac{\tau_x}{\tau_0}, \frac{\tau_y}{\tau_0}\right)$$

and introduce a barotropic stream function Ψ in the following way:

$$\bar{u}' = -\frac{1}{H'}\Psi_y, \quad \bar{v}' = \frac{1}{H'}\Psi_x.$$

Here L, H_m, U_0, ρ_0, p_0, τ_0 are representative values of length, depth, velocity, density, pressure, and wind tension, respectively, Ω_{pl} is the planetary vortex.

Then we differentiate equation (5) by y, deduct it from equation (6) differentiated by x and obtain a 2D nonlinear vorticity equation in terms of a stream function in the dimensionless form (dashes are omitted):

$$\frac{\partial}{\partial t}(\Delta_H\Psi) - \mathrm{rot}\left(\frac{1}{H}\Delta_H\Psi\,\nabla\Psi\right) - \frac{2\Omega_{pl}L}{U_0}\,\mathrm{rot}\left(\frac{f}{H}\nabla\Psi\right) + \frac{RL}{U_0}\Delta_H\Psi - \frac{\mu}{U_0 L}\Delta\Delta_H\Psi = F, \quad (8)$$

$$\operatorname{rot} U = -u_y + v_x, \quad \Delta_H \Psi = \Big(\frac{1}{H}\Psi_x\Big)_x + \Big(\frac{1}{H}\Psi_y\Big)_y, \quad F = \frac{\tau_0 L}{\rho_0 H_m U_0^2} \operatorname{rot} \frac{\tau}{H},$$

with boundary and initial conditions

$$\Psi|_{\partial\Omega} = 0, \quad \Delta_H \Psi|_{\partial\Omega} = 0, \quad \Psi|_{t=0} = \Psi^0(x, y).$$

In terms of vorticity $\zeta = \Delta_H \Psi$, equation (8) can be rewritten in the form

$$\zeta_t - \operatorname{rot}\Big(\frac{1}{H}\zeta \nabla\Psi\Big) - \frac{2\Omega_{pl} L}{U_0} \operatorname{rot}\Big(\frac{f}{H} \nabla\Psi\Big) + \frac{RL}{U_0}\Delta_H \Psi - \frac{\mu}{U_0 L}\Delta\zeta = F, \quad (9)$$

$$\Psi|_{\partial\Omega} = 0, \quad \zeta|_{\partial\Omega} = 0, \quad \zeta|_{t=0} = \Delta_H \Psi^0(x, y).$$

Let us divide the interval $[0, T]$ into N_t sub-intervals with a length h_t. According to a weak approximation method, problem (9) will be solved by splitting in terms of physical processes [4]:

Step I:

$$(\zeta_1)_t - \operatorname{rot}\Big(\frac{1}{H}\zeta_1 \nabla\Psi_2^n\Big) - \frac{\mu}{U_0 L}\Delta\zeta_1 = 0, \quad (10)$$

$$\zeta_1|_{\partial\Omega} = 0, \quad \zeta_1|_{t=t_n} = \Delta_H \Psi_2|_{t=t_n};$$

Step II:

$$(\Delta_H \Psi_2)_t - \frac{2\Omega_{pl} L}{U_0} \operatorname{rot}\Big(\frac{f}{H} \nabla\Psi_2\Big) + \frac{RL}{U_0}\Delta_H \Psi_2 = F, \quad (11)$$

$$\Psi_2|_{\partial\Omega} = 0, \quad \Delta_H \Psi_2|_{t=t_n} = \zeta_1|_{t=t_{n+1}};$$

$t \in [t_n, t_{n+1}]$, $n = 0, \ldots, N_t - 1$.

Here the first step describes the advection and diffusion of the vorticity and the second one is in solving the linear stream function equation with forcing.

2. Construction of schemes

In Ω, we construct a rectangular grid. Then rectangles of the grid are divided into triangles by diagonals with variable directions, either positive or negative (Figure 1).

Let us consider two types of finite elements:

- Conforming elements ω_{pq}^{c} are piecewise linear functions determined by values at vertices of triangles in the following way:

$$\omega^{\mathrm{c}}_{pq}(x_k, y_l) = \begin{cases} 1, & (k,l) = (p,q), \\ 0, & (k,l) \neq (p,q). \end{cases}$$

Here (x_k, y_l) is a vertex of a certain triangle of the grid.

- Non-conforming elements $\omega^{\mathrm{nc}}_{ij}$ are piecewise linear functions determined by values at midpoints of sides of triangles in the following way:

$$\omega^{\mathrm{nc}}_{ij}(x_k, y_l) = \begin{cases} 1, (k,l) = (i,j), \\ 0, (k,l) \neq (i,j). \end{cases}$$

Here (x_k, y_l) is a midpoint of a side of a certain triangle of the grid (Figure 2). Such functions were considered in [2, 5].

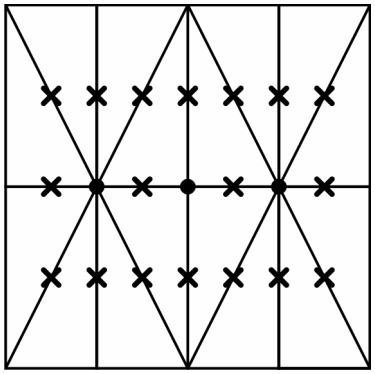

Figure 1. A fragment of the grid. Nodes • and × are associated with conforming and non-conforming finite elements, respectively

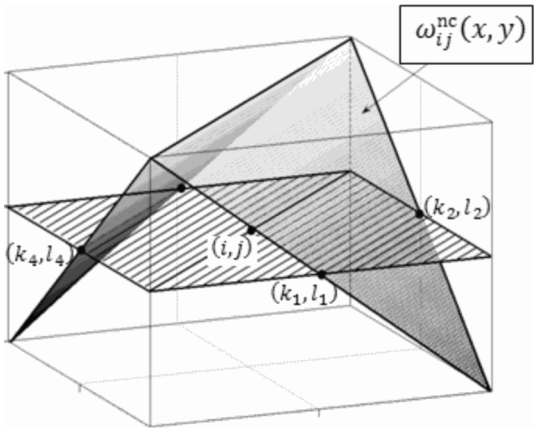

Figure 2. Non-conforming basis function

These functions possess some significant features: $\omega^{\mathrm{nc}}_{ij}$ are orthogonal and each conforming element ω^{c}_{pq} is a half-sum of the non-conforming ones surrounding it.

We will approximate the stream function Ψ_2 and the vorticity ζ_1 with linear combinations of conforming and nonconforming finite elements, respectively:

$$\Psi_2 \approx \psi^{N^{\mathrm{c}}} = \sum_{(p,q)\in N^{\mathrm{c}}} \psi_{pq}\, \omega^{\mathrm{c}}_{pq}(x,y),$$

$$\zeta_1 \approx \varphi^{N^{\mathrm{nc}}} = \sum_{(i,j)\in N^{\mathrm{nc}}} \varphi_{ij}(t)\, \omega^{\mathrm{nc}}_{ij}(x,y),$$

where N^{nc} is a set of mesh points including midpoints of the sides of triangles and N^{c} is a set of mesh points including triangles vertices; $\varphi_{ij}(t)$ and ψ_{pq} are weight coefficients to be determined.

Let us consider the splitting steps (10) and (11) in more detail. A weak formulation of the problem of the first splitting step (10) is the following:

$$((\zeta_1)_t, \omega) + I_1(\zeta_1, \omega) = 0 \quad \forall \omega \in \overset{\circ}{W}{}_2^1(\Omega), \;\; t \in (t_n, t_{n+1}], \tag{12}$$
$$(\zeta_1(x, y, t_n), \omega) = (\Delta_H \psi^{N^{\mathrm{c}}}, \omega) \quad \forall \omega \in \overset{\circ}{W}{}_2^1(\Omega),$$

where $\psi^{N^{\mathrm{c}}}$ is a conforming FEM solution of the second step (11) from the previous time layer.

Here $\overset{\circ}{W}{}_2^1(\Omega)$ is a subspace of $W_2^1(\Omega)$ which includes the functions vanishing at the boundary of the domain Ω;

$$I_1(u, v) = \int_\Omega \left(\frac{\mu}{U_0 L} u_x v_x + \frac{\mu}{U_0 L} u_y v_y + \psi^{N^{\mathrm{c}}} \left(\frac{1}{H} u \right)_x v_y - \psi^{N^{\mathrm{c}}} \left(\frac{1}{H} u \right)_y v_x \right) d\Omega.$$

There arises a problem when using the Bubnov–Galerkin method for the search for an FEM solution $\varphi^{N^{\mathrm{nc}}}$, which is a linear combination of non-conforming elements. The point is that when defining a weak solution, it is required to carry out the integral relation $\forall \omega \in \overset{\circ}{W}{}_2^1(\Omega)$ but the functions $\omega_{ij}^{\mathrm{nc}}(x, y)$ have discontinuities at the boundaries of their support. So, we need to introduce an approximate bilinear form

$$I_1^h(u, v) = \sum_k \int_{T^k} \left(\frac{\mu}{U_0 L} u_x v_x + \frac{\mu}{U_0 L} u_y v_y + \psi^{N^{\mathrm{c}}} \left(\frac{1}{H} u \right)_x v_y - \psi^{N^{\mathrm{c}}} \left(\frac{1}{H} u \right)_y v_x \right) d\Omega,$$

where T^k are triangles of the domain Ω. In this case, a non-conforming FEM solution $\varphi^{N^{\mathrm{nc}}}$ does not belong to the required space $\overset{\circ}{W}{}_2^1(\Omega)$ as well. However, if we assume that the function $H(x, y)$ is a step function on $\bigcup_k T^k$, then the efficiency of the scheme for the advection–diffusion problem similar to the presented one was verified earlier with the help of numerical experiments [6].

As a result, with allowance for orthogonality of non-conforming finite elements and their relation with the conforming ones, the following differential equation system is obtained:

$$M^h(\Phi)_t + \Lambda^h \Phi = 0, \quad t \in (t_n, t_{n+1}], \qquad \Phi|_{t=t_n} = X\overline{\Psi}. \tag{13}$$

Here $M^h = \mathrm{diag}(\theta_{ij}/3)$, $[\Lambda^h \Phi]_{ij} = I_1^h(\varphi^{N^{\mathrm{nc}}}, \omega_{ij}^{\mathrm{nc}})$, $[\Phi]_{ij} = \varphi_{ij}$, $[\overline{\Psi}]_{ij} = \psi_{ij}$, X is a transition matrix from the stream function to vorticity obtained from the relation between non-conforming and conforming elements, and θ_{ij} is an area of the support of the function $\omega_{ij}^{\mathrm{nc}}$.

In this case $\Lambda^h = S^h + K^h$, where S^h is a symmetric operator and K^h is a skew-symmetric operator corresponding to the symmetric and skew-symmetric parts of the integral operator.

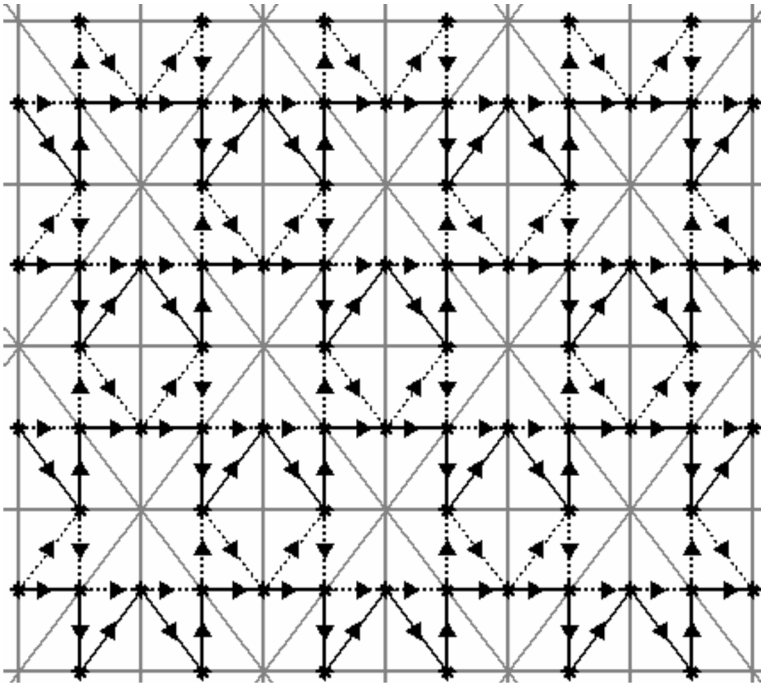

Figure 3. Direction of operators Λ_1^h (—) and Λ_2^h ($\cdots$)

Analysis of the operator Λ^h shows that it can be presented as a sum of two 1D positive semi-definite operators Λ_1^h and Λ_2^h acting along the broken lines connecting non-conforming mesh points (Figure 3). Moreover,

$$\Lambda_1^h = S_1^h + K_1^h, \qquad \Lambda_2^h = S_2^h + K_2^h,$$

where $S^h = S_1^h + S_2^h$, $K^h = K_1^h + K_2^h$, S_r^h are symmetric operators, K_r^h are skew-symmetric ones ($r = 1, 2$).

Such a decomposition of the grid operator allows the use of the splitting method with respect to time for solving problem (13). In this case, a two-cycle splitting method is used [7].

Let us divide the interval $[t_n, t_{n+1}]$ into sub-intervals $t_n + m\tau_1 \le t \le t_n + (m+1)\tau_1$, $\tau_1 = h_t/N_1$, $m = 0, \ldots, N_1 - 1$, N_1 is the number of additional time sub-intervals. The system of grid equations consists of a sequence of the Crank–Nicholson schemes for the operators Λ_1^h and Λ_2^h constructed on the sub-interval $[t_n + m\tau_1, t_n + (m+1)\tau_1]$:

$$\Big(M^h + \frac{\tau_1}{4}\Lambda_1^h\Big)\Phi^{m+1/4} = \Big(M^h - \frac{\tau_1}{4}\Lambda_1^h\Big)\Phi^m,$$

$$\Big(M^h + \frac{\tau_1}{4}\Lambda_2^h\Big)\Big(\Phi^{m+1/2} - \frac{\tau_1}{2}(M^h)^{-1} f^{m+1/2}\Big) = \Big(M^h - \frac{\tau_1}{4}\Lambda_2^h\Big)\Phi^{m+1/4},$$

$$\Big(M^h + \frac{\tau_1}{4}\Lambda_2^h\Big)\Phi^{m+3/4} = \Big(M^h - \frac{\tau_1}{4}\Lambda_2^h\Big)\Big(\Phi^{m+1/2} + \frac{\tau_1}{2}(M^h)^{-1} f^{m+1/2}\Big),$$

$$\Big(M^h + \frac{\tau_1}{4}\Lambda_1^h\Big)\Phi^{m+1} = \Big(M^h - \frac{\tau_1}{4}\Lambda_1^h\Big)\Phi^{m+3/4}.$$

To prove the approximation properties of the scheme with respect to time, the Taylor expansion in series with a restriction on the time space (14) is used:

$$\frac{\tau_1}{4}\big\|(M^h)^{-1}\Lambda_r^h\big\| \le 1. \tag{14}$$

In [7], it is shown that the method is absolutely stable.

After sampling the problem (11) with respect to time we have

$$\left(\frac{1}{h_t} + \frac{RL}{U_0}\right)\Delta_H\Psi_2^{n+1} + \frac{2\Omega_{pl}L}{U_0}\left(\frac{f}{H}\big(\Psi_2^{n+1}\big)_x\right)_y - \frac{2\Omega_{pl}L}{U_0}\left(\frac{f}{H}\big(\Psi_2^{n+1}\big)_y\right)_x = F + \frac{1}{h_t}\Delta_H\Psi_2^n$$

or, with allowance for the initial conditions,

$$\left(\frac{1}{h_t} + \frac{RL}{U_0}\right)\Delta_H\Psi_2^{n+1} + \frac{2\Omega_{pl}L}{U_0}\left(\frac{f}{H}\big(\Psi_2^{n+1}\big)_x\right)_y - \frac{2\Omega_{pl}L}{U_0}\left(\frac{f}{H}\big(\Psi_2^{n+1}\big)_y\right)_x = F + \frac{1}{h_t}\zeta_1^{n+1}. \tag{15}$$

After application of the Galerkin method to problem (15), a system of linear algebraic equations is obtained:

$$I_2\left(\psi^{N^{\mathrm{c}}}, \omega_{pq}^{\mathrm{c}}\right) = -\left(F, \omega_{pq}^{\mathrm{c}}\right) - \frac{1}{h_t}\left(\varphi^{N^{\mathrm{nc}}}, \omega_{pq}^{\mathrm{c}}\right), \quad (p,q) \in N^{\mathrm{c}}, \tag{16}$$

where

$$I_2(u,v) = \int\limits_\Omega \Bigg(\Big(\frac{1}{h_t} + \frac{RL}{U_0}\Big)\frac{1}{H}u_x v_x + \Big(\frac{1}{h_t} + \frac{RL}{U_0}\Big)\frac{1}{H}u_y v_y + \frac{2\Omega_{pl}L}{U_0}\frac{f}{H}u_x v_y - \frac{2\Omega_{pl}L}{U_0}\frac{f}{H}u_y v_x\Bigg)d\Omega,$$

$\varphi^{N^{\mathrm{nc}}}$ is a non-conforming FEM solution to problem (10).

System (16) is solved by an iterative technique.

3. Numerical experiments

The efficiency of the scheme was verified for each splitting step separately as well as for the whole problem. A circulation stabilization problem with a constantly acting force $F = \frac{\tau_0 L}{\rho_0 H_m U_0^2}\,\mathrm{rot}\,\frac{\tau}{H}$, a boundary layer, and a variable bottom is studied below.

For problem (8) we assume

$$\Omega = [0,1] \times \Big[0, yl = \frac{L_y}{L}\Big], \quad L = 4 \cdot 10^8 \text{ cm}, \quad L_y = 2 \cdot 10^8 \text{ cm},$$

$$f = \frac{f_0}{2\Omega_{pl}} + \frac{\beta L}{2\Omega_{pl}}(y - yl), \quad f_0 = 9.3 \cdot 10^{-5} \text{ s}^{-1}, \quad \beta = 1.88 \cdot 10^{-13} \,(\text{cm} \cdot \text{s})^{-1},$$

$$\Omega_{pl} = 7.3 \cdot 10^{-5} \text{ s}^{-1}, \quad \rho_0 = 1 \frac{\text{g}}{\text{cm}^3}, \quad F = -\frac{\pi \tau_0 L}{\rho_0 H_m U_0^2 yl} \frac{1}{H} \sin \frac{\pi y}{yl}, \quad \Psi^0 = 0.$$

Relative errors

$$\text{e}_{\text{rel},1} = \frac{\max\limits_{(p,q)\in N^{\text{c}}} |(\psi_{pq})^{n+1} - (\psi_{pq})^{n}|}{\max\limits_{(p,q)\in N^{\text{c}}} |(\psi_{pq})^{n+1}|},$$

$$\text{e}_{\text{rel},100} = \frac{\max\limits_{(p,q)\in N^{\text{c}}} |(\psi_{pq})^{n+1} - (\psi_{pq})^{n-99}|}{\max\limits_{(p,q)\in N^{\text{c}}} |(\psi_{pq})^{n+1}|},$$

a maximum of the FEM solution $\text{MAX} = \max\limits_{(p,q)\in N^{\text{c}}} |(\psi_{pq})^{n+1}|$ and its form are the results of the tests with the parameters specified below.

Test 1. For the flat bottom $H = 1$, $h_t = 10^{-4}$:

a) $\tau_0 = 1.0$ dyne/cm^2, $U_0 = 0.27$ cm/s, $\mu = 1.2 \cdot 10^9$ cm^2/s, $R = 5 \cdot 10^{-7}$ s^{-1}. One can observe a predominance of the west boundary layer which is typical of the Stommel model.

b) $\tau_0 = 1.0$ dyne/cm^2, $U_0 = 0.27$ cm/s, $\mu = 1.2 \cdot 10^8$ cm^2/s, $R = 5 \cdot 10^{-8}$ s^{-1}. In this case a weak influence of nonlinearity can be observed.

c) $\tau_0 = 1.0$ dyne/cm^2, $U_0 = 0.27$ cm/s, $\mu = 1.2 \cdot 10^7$ cm^2/s, $R = 5 \cdot 10^{-8}$ s^{-1}. A predominance of the nonlinear part of the equation results in clearly defined inertial boundary layer.

The results of the tests are shown in Table 1 and Figure 4.

At a fixed moment T, the results for schemes with different time steps h_t coincide with one another except for a minor difference in maxima of solutions, which is also in favor of convergence of the method. It is worth to note that the kind of the result corresponds fairly well to the current numerical solution of the problem in question.

Table 1. Velocity of stabilization and a maximum of FEM solution with respect to the number of time steps

The number of time steps (corresponding time, years)	Test 1a		Test 1b		Test 1c	
	$e_{rel,1}$ ($e_{rel,100}$)	MAX	$e_{rel,1}$ ($e_{rel,100}$)	MAX	$e_{rel,1}$ ($e_{rel,100}$)	MAX
10 (0.47)	$2.3 \cdot 10^{-2}$	5.09	$5.1 \cdot 10^{-2}$	6.84	$9.5 \cdot 10^{-2}$	6.82
50 (2.38)	$5.5 \cdot 10^{-6}$	5.403	$5.8 \cdot 10^{-5}$	7.05	$1.8 \cdot 10^{-2}$	12.7
300 (14.3)	$2.0 \cdot 10^{-9}$ ($2.2 \cdot 10^{-7}$)	5.403	$4.9 \cdot 10^{-9}$ ($8.7 \cdot 10^{-7}$)	7.05	$1.2 \cdot 10^{-6}$ ($1.4 \cdot 10^{-4}$)	13.04
500 (23.84)	$6.2 \cdot 10^{-10}$ ($9.8 \cdot 10^{-8}$)	5.403	$3.1 \cdot 10^{-9}$ ($3.9 \cdot 10^{-7}$)	7.05	$3.5 \cdot 10^{-8}$ ($1.2 \cdot 10^{-6}$)	13.04
1000 (47.69)	$1.9 \cdot 10^{-11}$ ($3.0 \cdot 10^{-9}$)	5.403	$7.4 \cdot 10^{-11}$ ($1.4 \cdot 10^{-8}$)	7.05	$7.4 \cdot 10^{-10}$ ($5.6 \cdot 10^{-8}$)	13.04
1500 (71.53)	$1.0 \cdot 10^{-12}$ ($8.7 \cdot 10^{-11}$)	5.403	$1.0 \cdot 10^{-12}$ ($1.3 \cdot 10^{-10}$)	7.05	$1.2 \cdot 10^{-10}$ ($1.1 \cdot 10^{-8}$)	13.04
2000 (95.38)	$1.0 \cdot 10^{-14}$ ($2.0 \cdot 10^{-12}$)	5.403	$1.0 \cdot 10^{-14}$ ($1.0 \cdot 10^{-12}$)	7.05	$3.3 \cdot 10^{-11}$ ($3.7 \cdot 10^{-8}$)	13.04

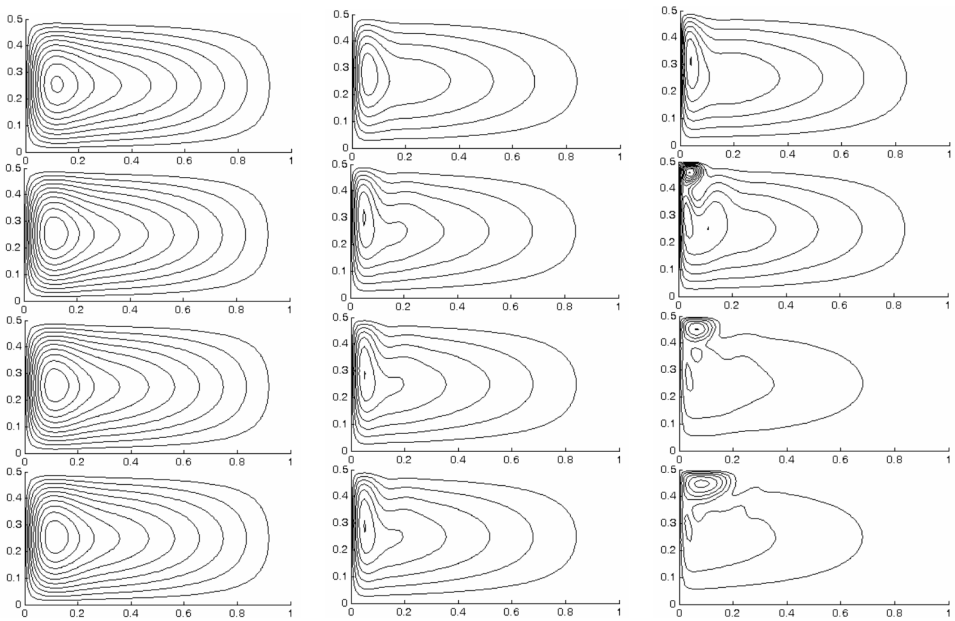

Test 1a Test 1b Test 1c

Figure 4. Stabilization of the FEM solution for the flat bottom with respect to the number of time steps $[100 \times 50 \times N_t]$. From top to bottom $N_t = 10$, 20, 30, 300

Test 2. For the variable bottom with parameters $\tau_0 = 1.0$ dyne/cm^2, $U_0 = 0.27$ cm/s, $\mu = 1.2 \cdot 10^9$ cm^2/s, $R = 5 \cdot 10^{-7}$ s^{-1}, $h_t = 10^{-4}$, the results fit well with the theory that claims the dependence between a sign of the derivative $\frac{\partial}{\partial y}\left(\frac{f}{H}\right)$ and the intensification zone [8] (Figure 5). In the tests:

a) $H = \frac{\exp^{1.3y}}{\exp^{1.3y_l}}$. The negative sign implies eastward intensification.

b) $H = \frac{1}{H_m}\left(\frac{(x-1/2)^2}{2p} - \frac{(y-y_l/2)^2}{2q} - \frac{H_m}{10}m\right)$, $p = \frac{1}{8(H_m/10 - H_0)}$, $q = \frac{y_l^2}{8(H_m - H_m/10)}$, $H_0 = 4 \cdot 10^2$. The derivative changes a sign that results in two intensification zones.

The results of the tests are shown in Table 2.

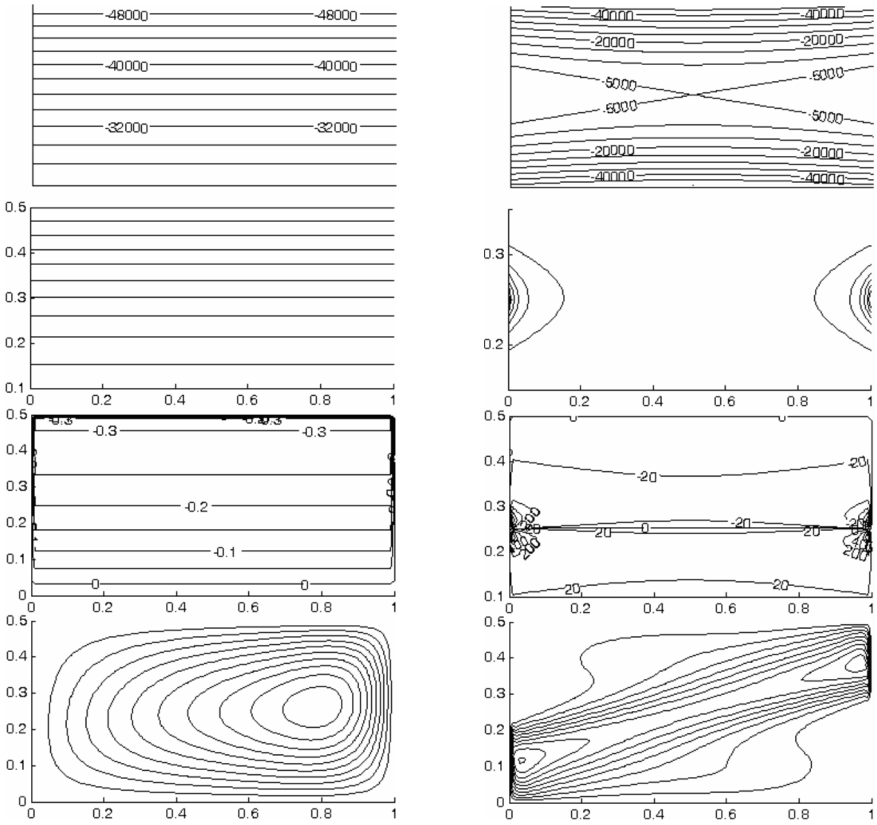

Figure 5. The dependence between a sign of the derivative $\partial(f/H)/\partial y$ and the intensification zone. From top to bottom: relief of the bottom, function f/H, derivative $\partial(f/H)/\partial y$, FEM solution for the variable bottom at the moment of time corresponding $N_t = 500$

Table 2. Velocity of stabilization and a maximum of FEM solution with respect to the number of time steps

The number of time steps (corresponding time, years)	Test 2a		Test 2b	
	$e_{rel,1}$ ($e_{rel,100}$)	MAX	$e_{rel,1}$ ($e_{rel,100}$)	MAX
10 (0.47)	$6.5 \cdot 10^{-2}$	6.906	$5.0 \cdot 10^{-4}$	0.5
50 (2.38)	$5.5 \cdot 10^{-5}$	10.66	$4.2 \cdot 10^{-7}$	0.5
300 (14.3)	$6.3 \cdot 10^{-9}$ ($7.0 \cdot 10^{-7}$)	10.66	$9.0 \cdot 10^{-13}$ ($1.2 \cdot 10^{-10}$)	0.5
500 (23.84)	$4.3 \cdot 10^{-9}$ ($4.7 \cdot 10^{-7}$)	10.66	$< 10^{-13}$ ($< 10^{-12}$)	0.5
1000 (47.69)	$1.8 \cdot 10^{-9}$ ($2.0 \cdot 10^{-7}$)	10.66	$< 10^{-13}$ ($< 10^{-12}$)	0.5
1500 (71.53)	$8.0 \cdot 10^{-10}$ ($8.6 \cdot 10^{-8}$)	10.66	$< 10^{-13}$ ($< 10^{-12}$)	0.5
2000 (95.38)	$3.5 \cdot 10^{-10}$ ($3.5 \cdot 10^{-8}$)	10.66	$< 10^{-13}$ ($< 10^{-12}$)	0.5

Conclusion

Based on the splitting in terms of physical processes and with respect to time and on a finite element method as applied to a 2D nonlinear vorticity equation in a rectangular basin with variable depth, a scheme with two splitting steps was obtained. At the first splitting step, for solving the linear stream function equation, conforming piecewise-linear finite elements are used. At the second step, corresponding to the vorticity advection and diffusion, non-conforming finite elements are used. Such elements allow the reduction of the number of grid points in a numerical scheme and presentation of a grid operator as two 1D positive semi-definite operators thus reducing the time needed for successive splitting with respect to time. The efficiency of the scheme was tested for each splitting step separately as well as on the problem as a whole.

References

[1] Crouzeix M., Raviart P.A. Conforming and non-conforming finite element methods for solving the stationary Stokes equations // R.A.I.R.O., (R-3). — 1973. — P. 33–75.

[2] Hua B.-L., Thomasset F. A noise-free finite element scheme for the two-layer shallow water equations // Tellus. — 1984. — Vol. 36 A. — P. 157–165.

[3] Kuzin V.I. Finite Element Method in Simulation of Oceanic Processes. — Novosibirsk: VC SO AN SSSR, 1985 (In Russian).

[4] Marchuk G.I. Splitting-up Methods. — Moscow: Nauka, 1988.

[5] Kuzin V.I., Moiseev V.M. Numerical scheme with the using of non-conforming finite elements for the search for a barotropic component of a current // Matematicheskoe modelirovanie dinamicheskih protsessov v okeane. — Novosibirsk, 1987. — P. 29–51 (In Russian).

[6] Kuzin V.I., Kravtchenko V.V. Application of non-conforming finite elements for solving problems of diffusion and advection // Siberian J. Num. Math. / Sib. Branch of Russ. Acad. of Sci. — Novosibirsk, 2010. — Vol. 13, No. 1. — P. 51–65.

[7] Marchuk G.I., Kuzin V.I. On a combination of finite element and splitting-up methods in the solution of parabolic equations // J. Comput. Phys. — 1983. — Vol. 52, No. 2. — P. 237–272.

[8] Welander P. Wind-driven circulation in one and two layer oceans of variable depth // Tellus. — 1968. — Vol. 20, No. 1. — P. 1–16.